Available online at www.sciencedirect.com

ScienceDirect

journal homepage: www.elsevier.com/locate/he

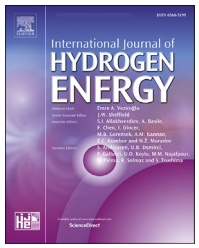

The regulation effect of methane and hydrogen on the emission characteristics of ammonia/air combustion in a model combustor

Meng Zhang [a,*], *Zhenhua An* [a], *Liang Wang* [b], *Xutao Wei* [a], *Bieerlan Jianayihan* [b], *Jinhua Wang* [a], *Zuohua Huang* [a], *Houzhang Tan* [c]

[a] *State Key Laboratory of Multiphase Flow in Power Engineering, Xi'an Jiaotong University, Xi'an 710049, China*
[b] *Xinjiang Uygur Autonomous Region Inspection Institute of Special Equipment, Urumqi 830011, China*
[c] *MOE Key Laboratory of Thermo-Fluid Science and Engineering, Xi'an Jiaotong University, Xi'an 710049, China*

HIGHLIGHTS

- The regulation effects of methane and hydrogen on NOx emission of ammonia/air flames in a swirl combustor are investigated.
- The emission characteristics are verified similar between 1D simulation and the experimental results.
- The flame structure detected by OH-PLIF is used to reveal NO emission qualitatively.
- The relation of NO and OH is revealed by LES for the NH_3/CH_4/air flame.

ARTICLE INFO

Article history:
Received 23 December 2020
Received in revised form
24 March 2021
Accepted 25 March 2021
Available online 23 April 2021

Keywords:
Ammonia
Methane
Hydrogen
NOx
Emission characteristics
Swirl flame

ABSTRACT

Ammonia, made up of 17.8% hydrogen, has attracted a lot of attention in combustion community due to its zero carbon emission as a fuel in gas turbines. However, ammonia combustion still faces some challenges including the weak combustion and sharp NOx emissions which discourage its application. It was demonstrated that the combustion intensity of ammonia/air flame can be enhanced through adding active fuels like methane and hydrogen, while the NOx emission issue will emerge in the meantime. This study investigates regulation effect of methane and hydrogen on the emission characteristics of ammonia/air flame in a gas turbine combustor. The instantaneous OH profile and global emissions at the combustion chamber outlet are measured with Planar Laser Induced Fluorescence (PLIF) technique and the Fourier Transform Infrared (FTIR), respectively. The flames are also simulated by large eddy simulation to further reveal physical and chemical processes of the emissions formation. Results show that for NH_3/air flames, the emissions behavior of the gas turbine combustor is similar to the calculated one-dimensional flames. Moreover, the NOx emissions and the unburned NH_3 can be simultaneously controlled to a proper value at the equivalence ratio (φ) of approximate 1.1. The variation of NO and NO_2 with φ for NH_3/H_2/air flames and NH_3/CH_4/air flames at blending ratio (Z_f) of 0.1 are similar to the NH_3/air flames, with the peak moving towards rich condition. This indicates that the NH_3/air flame can be regulated through adding a small amount of active fuels without increasing the NOx emission level. However, when $Z_f = 0.3$, we observe a clear large NOx emission and CO for NH_3/CH_4/air flames, indicating H_2 is a better choice on the emission control. The LES results show that NO and OH radicals exhibit a general positive

* *Corresponding author.*
E-mail address: mengz8851@xjtu.edu.cn (M. Zhang).
https://doi.org/10.1016/j.ijhydene.2021.03.210

correlation. And the temperature plays a secondary role in promoting NOx formation comparing with CH_4/air flame.

Nomenclature

A	area of the OH-PLIF images
D_i/D_o	inner/outer diameter of the swirler
F	thicken factor
HRR	heat release rate
I_{OH}	OH-PLIF intensity
I_{ave}	averaged OH intensity
N	number of the averaged OH-PLIF images
Q_f	volume rate of CH_4/H_2
Q_{NH3}	volume rate of NH_3
S	swirl number
S_L	laminar flame speed
U	inlet velocity
Y_i	mass fraction of species i
Z_f	blending ratio of CH_4/H_2
Ξ_Δ	wrinkling factor
φ	equivalence ratio

Introduction

As the increasing threat of global warming, a green (low/zero-carbon) economy concept is considered as a future choice for the power of vehicles, the industrial combustion devices and the power plants. Recent researches on ammonia (NH_3) combustion rose the opportunity of extensively reducing the greenhouse gas (CO_2) [1,2], since it is not only a suitable hydrogen carrier but also is a carbon-free molecule burned without carbon dioxide emissions (CO_2) [3–5]. Moreover, there are well-established, reliable infrastructures for both ammonia storage and distribution globally. Therefore, the application of ammonia as the chemical storage of energy to replace fossil fuels has recently attracted a lot of research interests and becomes a main objective for the research groups in this field [4–6], especially in gas turbines.

However, investigations [1] show that there are two primary challenges which discourage the application of fuelling ammonia on the combustion devices. Firstly, the flame speed of the premixed ammonia/air flame (the NH_3/air flame) is extremely low, i.e., about one-fifth of methane/air (CH_4/air) mixture at the stoichiometric ratio condition, which means the flame is prone to blow-off and thus results in a very limited flame stabilization range [7]. Nevertheless, Hayakawa et al. [7] proved that the NH_3/air flame has a limited flame stable range in a swirl combustor without any addictives. Previous studies show that the stabilization can be enhanced and the stable range can be extended by blending the active fuels like methane and hydrogen [8–10]. Secondly, contrary to CH_4/air flame, NH_3/air flame emits high NOx especially at lean conditions [3,5,11]. And the NOx concentration is found even higher when adding methane into ammonia as the addictive [9,12], especially at fuel lean conditions. This means the premixed lean combustion concept is not an suitable strategy for ammonia containing fuel. For example, when methane is added to NH_3/air flame, the O, H and OH radical concentration becomes higher resulting in the increasing of NOx production because the NO forming route through oxidation of NH_2 and NH is promoted [13]. The simulation from one dimensional laminar flame indicates that the production of NOx will be largely increased even adding 10% CH_4 into NH_3 fuel by volume [14]. Therefore, the NOx control becomes the key issue for the ammonia combustion community.

Numerous researches have been conducted on the emission characteristics for the ammonia containing fuel. Okafor et al. [3] developed a micro gas turbine (MGT) combustor for developing efficient combustion and low NOx emission of pure ammonia. Their results demonstrated that NOx emission is primarily depended on the equivalence ratio upstream of the combustor. In addition, there exists an optimal equivalence ratio where the main emissions reach the minimum. Jójka and Slefarski [15] investigated the NO formation of CH_4/NH_3/air flames in a nozzle burner with the NH_3 content in the fuel from 1% up to 5%. NO is found increasing with the NH_3 content in the fuel, i.e., 2000 ppmv at 5% NH_3 in their results. Okafor et al. [9] also investigated the emission characteristics of the co-firing flames with the ammonia heat fraction in the fuel up to 0.3 (mole fraction of 50%) in their MGT combustor. The NOx emissions in the single-stage combustion can be twice compared with their already reported values for NH_3/air flames. Medina et al. [5] studied the optimisation of fuel injection and flame stabilization in a tangential swirl burner with ammonia as the primary fuel with the NH_3 mole fraction of 69%. They found the NOx concentration is about 3000 ppmv at lean condition and they suggested that a fully premixed injection can be a potential way to reduce NOx formation. Ramos et al. [16] measured emissions from a laminar flame of the NH_3/CH_4 co-fired fuel. The NH_3 molar fraction in the fuel mixture was varied up to 70%. The experimental results showed that the NOx concentration initially increases as the fraction of NH_3 in the fuel mixture rises up to 0.5, decreasing afterwards. Furthermore, NOx emissions decrease as the equivalence ratio reducing towards fuel-lean conditions.

As one kind of fuels, ammonia is a very important branch in the hydrogen economy due to its merits. And the final goal is the pure ammonia burning in the combustion device to realize zero CO_2 emission. Therefore, the emission characteristics of pure ammonia or the regulated ammonia combustion, i.e., by small amount of methane/hydrogen, should

be largely investigated. However, ammonia has not been used as a fuel until past few years. The previous work, especially the experimental researches on swirl combustor, mainly treats NH_3 as the addictive and the NH_3 ratio is limited, i.e., the maximum mole fraction in the fuel is 70%. To this end, the current study focus on the emission characteristics of the NH_3/CH_4/air and NH_3/H_2/air co-firing flames in a model gas turbine combustor, with the CH_4/H_2 mole fraction limited to 0.3. To identify the flame structure, the OH profile diagnosis is performed through laser diagnostics technique of Planar Laser Induced Fluorescence (PLIF). The global emissions at combustion chamber outlet are measured with the Fourier Transform Infrared (FTIR). The hot gas velocity field is measured by particle imaging velocimetry (PIV). Large eddy simulation with detailed chemistry using OpenFOAM is conducted to further explaining the experimental results from an insight of the emission chemical production.

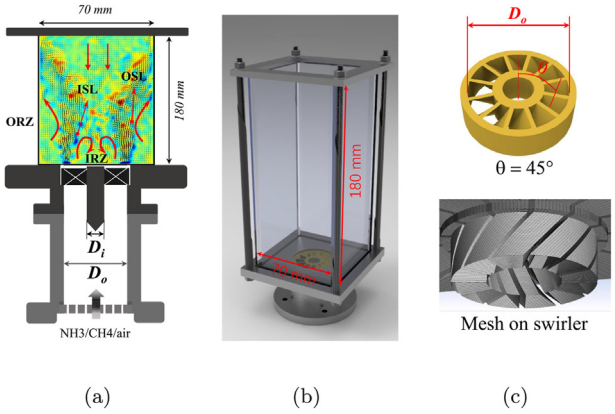

Fig. 1 – (a) The schematic of the combustor; (b) the geometry and dimension of the combustion chamber; (c) the geometry and mesh of the swirler.

Experimental setup and the methodologies

The combustor

The swirl flame is stabilized in a stainless steel, full premixed combustor, which was already introduced in our previous research [17]. It is only briefly described here to facilitate the understanding. The current burner is updated based on our bluff body and swirl combustor in Ref. [18]. Since the main geometry is similar, only the head section and the swirler are shown in Fig. 1. The bluff body is unmounted in the current burner and the swirler is updated to 12 vanes which is installed at the burner exit, as shown in Fig. 1(b) and (c). The swirl flame is stabilized inside a squared combustion chamber with dimension of 70 × 70 × 180 mm^3. The chamber wall is made of quartz glass to allow laser diagnostics, as shown in Fig. 1(b). The swirl number S, representing the ratio of the axial flux of angular momentum to axial momentum, which can be evaluated by $S = \frac{2}{3}\frac{1-(D_i/D_o)^3}{1-(D_i/D_o)^2}\tan\theta$ [19].

Liquid ammonia is vaporized to gas phase through pressure reducing valve. The compressed high purity (>99.9%) hydrogen/methane are injected to the main fuel pipe as the additives. The fuel and air are fully mixed at the mixing chamber before supplying to the combustor. The blending ratio of additives in ammonia Z_f (CH_4/H_2) is defined by its mole fraction in the fuel as $Z_f = Q_f/(Q_f + Q_{NH_3})$. Q_f and Q_{NH_3} are the volume flow rate of CH_4/H_2 and NH_3, respectively. The operating conditions are shown in Table 1. The blending ratios $Z_f = 0$, 0.1 and 0.3 are investigated for both NH_3/CH_4/air and NH_3/H_2/air flames. For brevity, we will use the abbreviation of each flame in the coming sections, as designated in Table 1. The emission characteristics within the stabilized range are studied at the fixed inlet velocity of 3 m/s for all cases.

The laser diagnostics

The instantaneous velocity field and OH species profile are measured by particle imaging velocimetry (PIV) and planar laser induced fluorescence (OH-PLIF) technique respectively [17]. The details of the PIV system is presented in out previous work [8,20], which is not introduced here. The OH-PLIF system includes a Nd:YAG laser (Quanta-Ray Pro-190), a pumped dye laser (Sirah PRSC-G-3000) and an ICCD camera (LaVision Image ProX) with software for signal control and data acquisition. The Nd:YAG laser source generates the raw laser with the wavelength of 532 nm at the repetition rate of 10 Hz and the energy of 0.5 J per pulse. The laser frequency is doubled with the pumped dye laser (SirahPRSC-G-3000) and the laser is transferred to 282.769 nm to excite the Q1(8) line of the $A2\Sigma \leftarrow X2\sigma$ (1,0) transition. The fluorescence is acquired by an ICCD camera through a UV lens (Nikon Rayfact PF 10545 MF-UV) and OH bandpass filtered (LaVision VZ08-0222) with intensified Relay Optics (LaVision VC08-0094) at gate with of 100 ns. The resolution of the ICCD is 1200 × 900 pixels for viewing the flame with spatial resolution of 0.14 mm/pixel. The line-of-sight chemiluminiscence flame images are recorded by a Cannon X5 camera with a prime lens (EF 50 mm, f/1.4 USM). The aperture is set as $f = 1.4$ and the exposure time is set at 1/4 s to capture the mean flame structures.

Exhaust gas analysis

The Gasmet DX4000 Fourier Transform Infrared (FTIR) gas analyzer with a Gasmet Portable Sampling System (PSS) is employed to measure the global NOx and other emission concentrations at the combustor outlet. Fig. 2 shows the FTIR system and the schematic of the measurement. The sample gas pumped to PSS can be measured without drying since the sample pump, heated filter and valve are all located in a module that is heated to 453 K. This ensures that the sample stays in gaseous phase even with high concentrations of H_2O or corrosive gases. Before each series of measurements, the zero point calibration can be done automatically by PSS with nitrogen. The exhaust gas simple probe is placed 150 mm above the burner. To avoid the residual gas, i.e. CO, CO_2 or NH_3 of other cases in the sampling cell, the data is logged for a relatively long time after refreshed by nitrogen. The data is logged for about 180 s for near stoichiometric conditions and for 300 s for lean and rich conditions until the value for each component approached steady state. The average of the

Table 1 – The parameters of the mixtures.

Composition	CH_4/H_2 ratio vol-%	Abbreviation	φ	U_{max} (m/s)	Vane angle
NH_3/air	0	NH_3	0.7–1.3	3	45°
NH_3/CH_4/air	10,30	10%CH_4, 30%CH_4	0.7–1.4	3	45°
NH_3/H_2/air	10,30	10%H_2, 30%H_2	0.7–1.4	3	45°

collected data is regarded as the global emission value. The uncertainties are no larger than 50 ppmv when the measuring range is 5000 ppm (NO, NH_3), while it is under 2% for CO and CO_2. However, the uncertainties is less than ±10 ppm for N_2O and NO_2 since the measuring range is less than 200 ppm. We tested the repeatability before the experiments and the relative error of the measurement is below 5% for the major species for the tested mixture. The inlet velocity U is adjusted to a stable value (3 m/s) during the measurement to make sure the enough measurement time for the FTIR analysis.

Large eddy simulation

Large eddy simulation (LES) with finite rate chemistry is performed on the same geometry as the experiments to further reveal the emission features. The simulations solve the filtered 3D unsteady conservation equations of mass, momentum, energy as well as the state equation. A dynamic thinkened flame (DTF) model is applied by artificially thickening the flame with a factor of F while keeping the laminar flame speed S_L unchanged. A sub-grid flame wrinkling factor Ξ_Δ base on fractal theory is used to compensate the lost flame surface due to the thickening process. The chemical source term and the diffusion term are modified by F and Ξ_Δ. In the TDF model, we use a sensor defined by the temperature to identify the flame region where the thickening process should be applied ($F = 3$ in this study). And then $F = 1$ was set in the rest regions to keep the high fidelity of the simulation. Details of the DTF model and the numerical methodology can be found in Refs. [21,22].

The combustion chamber is meshed based on the computational accuracy requirement. The finest grid space of 0.2 mm is applied near the flame location. To preferably capture the swirl flow generated by the swiler, the geometry of an axial swirler with 12 vanes and 45° vane angle is also meshed, as shown in Fig. 1(c). The overall computational domain including the chamber and the swirler is divided into about 5 million structured grids. The inlet boundary is set based on the mass flow rate according to the experimental conditions. Isothermal wall of 750 K and non-slip boundary conditions are applied at chamber side walls. Pressure outlet boundary condition is applied at the combustion chamber exit. The temperature of the inlet mixture is 300 K and the ambient pressure is 1.0 atm. Before performing the LES of combustion, the current mesh has been tested satisfied for the grid convergence. In LES simulation, the mechanism of Xiao et al. [23] with 31 species and 243 reactions is employed owing to its small size. With the current computational setup, every case needs roughly 120,000 CPU hours. The emission properties for ammonia/methane/air mixtures, including NOx, HCN, CO and CO_2 are calculated with 1D laminar flame and the reaction mechanism developed by Okafor et al. [24] using ANSYS Chemkin-PRO [25]. The prediction ability on the emission of the mechanisms developed by Okafor et al. [24] and Xiao et al. [23] was verified similar.

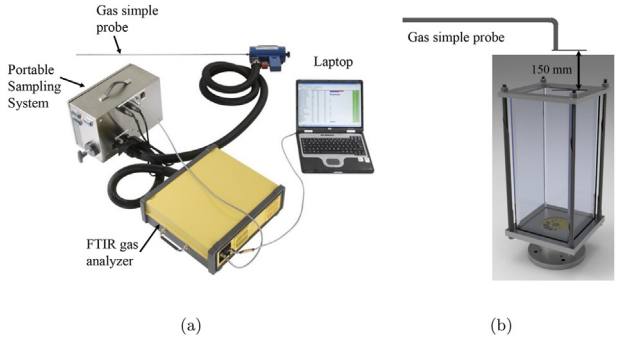

Fig. 2 – (a) The Fourier Transform Infrared gas analyzer system and (b) the schematic of the measurement.

Results and discussions

Flame structure - direct images

Fig. 3 shows the direct digital flame images of NH_3 flame and the 10%CH_4 flame with equivalence ratio φ. The images of 30% CH_4 flame, 10%H_2 flame and 30%H_2 flame are not shown here due to brevity since these flames behave similarly. The mixture inlet velocity is $U = 3.0$ m/s. From Fig. 3, we can clearly see a different behavior of the flame macro structure with φ when adding a small amount of methane as the addictive. The NH_3 flame reveals the orange chemiluminescence which induced by the $NH_2\alpha$ band spectrum and superheated water vapor spectrum [26]. It can be observed that the orange chemiluminescence is decreased and the flame is shortened when 10% CH_4 is added into the pure NH_3 flame. The inside of the liner is filled with NH_3 flame and the chemiluminescence could be observed even downstream of the combustion chamber outlet. It is also readily seen that the lean stabilization limit is extended by the CH_4 addition. The flame structure of the co-firing flames can be further revealed by the OH-PLIF images in the following section.

The flame OH profile

The profile of the instantaneous OH concentration is proved similar to the NO concentration for premixed NH_3/CH_4 co-firing flame by Okafor et al. [9]. The simultaneous measurement of the OH and NO profile shows that the high local OH

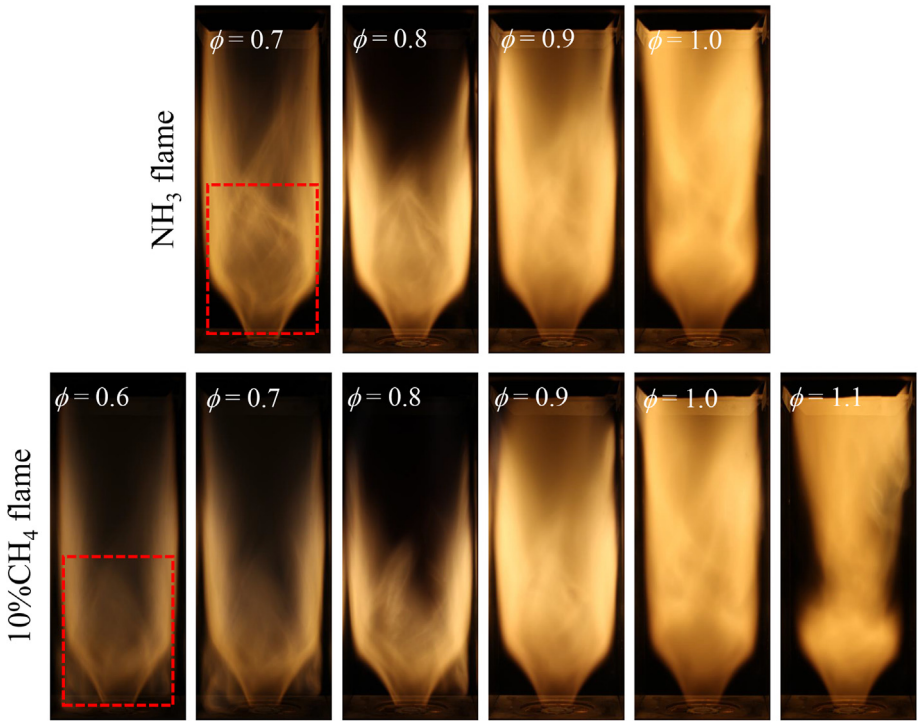

Fig. 3 – Direct flame images for NH_3 flame and 10%CH_4 flame with equivalence ratio. The red dashed box shows the PLIF view window. (For interpretation of the references to colour in this figure legend, the reader is referred to the Web version of this article.)

concentration regions corresponds to high NO-PLIF intensity. In addition, they also showed that the measured NO emissions follows the trend of plane-integrated time-averaged OH-PLIF intensities for both premixed and non-premixed conditions. Furthermore, Somarathne et al. [27] investigated the correlation of NO and OH for fuel-lean, stoichiometric and fuel-rich case by LES. A clear linear correlation between NO and OH is observed for NH_3 flame at all conditions, while the NO–OH distribution for CH_4/air flames is only positively correlated. Therefore, we performed the OH-PLIF measurement to indicate the NO field and to reveal the regulation effect of methane and hydrogen on ammonia combustion using the plane-integrated time-averaged OH-PLIF intensities.

The instantaneous and mean OH-PLIF images of the NH_3 flame, 10%CH_4 flame, 30%CH_4 flame at various equivalence ratios are shown in Fig. 4. Both instantaneous and mean images illustrate the flame structure. As we analysed earlier, the averaged OH profile highlights the distribution of OH intensity or OH concentration in the measurement plane. Moreover, the sharp increase of OH intensity can be regarded as the flame location for the premixed flame [17,28]. When surveying Fig. 4(a), the OH intensity is found higher at flame location (brighter region), where the OH radical concentration is large. We can see that the OH intensity seems to reach its highest value around $\varphi \approx 0.8$, which is close to the equivalence ratio corresponding the peak NO emission in the next section. And the OH intensity is decreasing when the mixture either goes richer or leaner. In the figure, the OH-PLIF image is shown only to $\varphi = 1.1$ because the OH intensity is too low for $\varphi > 1.1$. The time-averaged OH-PLIF images of 500 single shots are also shown in Fig. 4(b). The peak of the OH intensity is not corresponding to the stoichiometric ratio ($\varphi = 1.0$). For the cases tested in the current study, the peak intensity is bias to lean condition. The methane addition can enhance the mean OH intensity and the enhancement is more evident at methane blending ratio of 30%.

The variation of the mean OH intensity with equivalence ratio can be demonstrated with the plane-integrated time-averaged OH intensity I_{ave}, which is defined as

$$I_{ave} = \frac{\sum_{n=1}^{N} \int I_{OH} dA}{N \cdot A} \quad (1)$$

where I_{OH} is the local OH intensity, A represents the integral area and N is the total number of the averaged images. In the current study, I_{ave} is obtained by averaging the integration of the OH signal counts of 500 instantaneous OH-PLIF images. The variation of I_{ave} with the equivalence ratio is shown in Fig. 5 for both NH_3/CH_4/air flame and NH_3/H_2/air flame. The error bar gives the standard deviation of the data. The intensity of OH-PLIF image is largely depend on the laser excitation energy, excitation laser wavelength and the camera settings. And the difference of the flame temperature barely influences the absorption spectrum. Therefore, the major difference of the I_{ave} comes from the OH intensity of the flame itself. And the qualitative trends of OH concentration with φ can be revealed by the mean OH-PLIF images once we use the same experimental settings. I_{ave} also shows the qualitative behavior of NO since NO has a linear relation and NO production is facilitated by the OH concentration in ammonia containing flames [9].

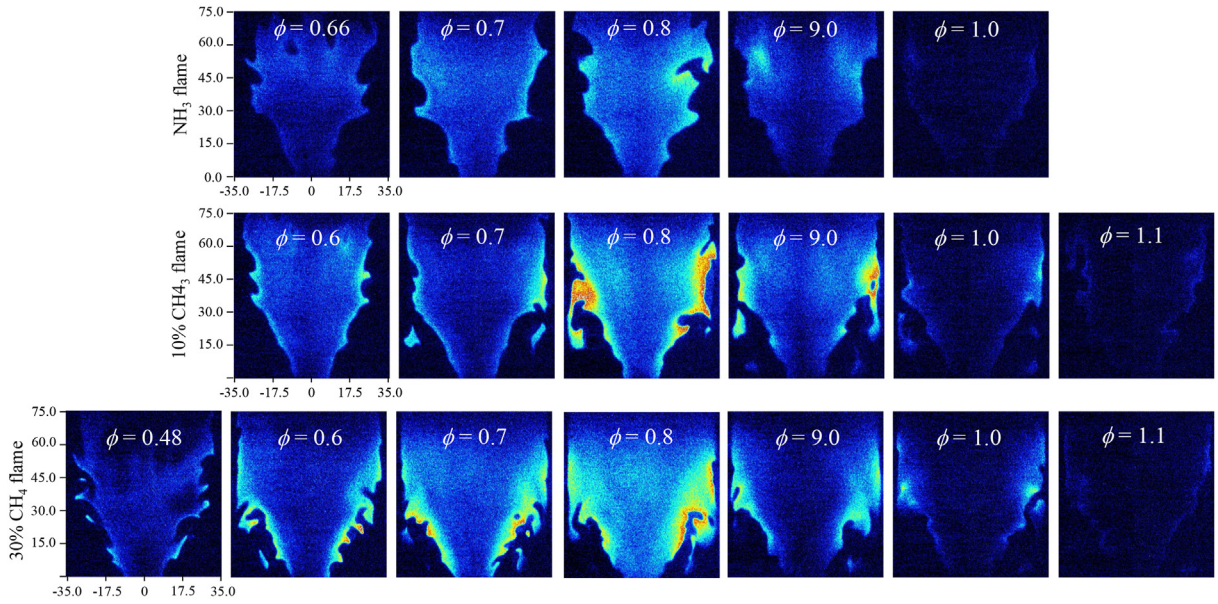

(a)

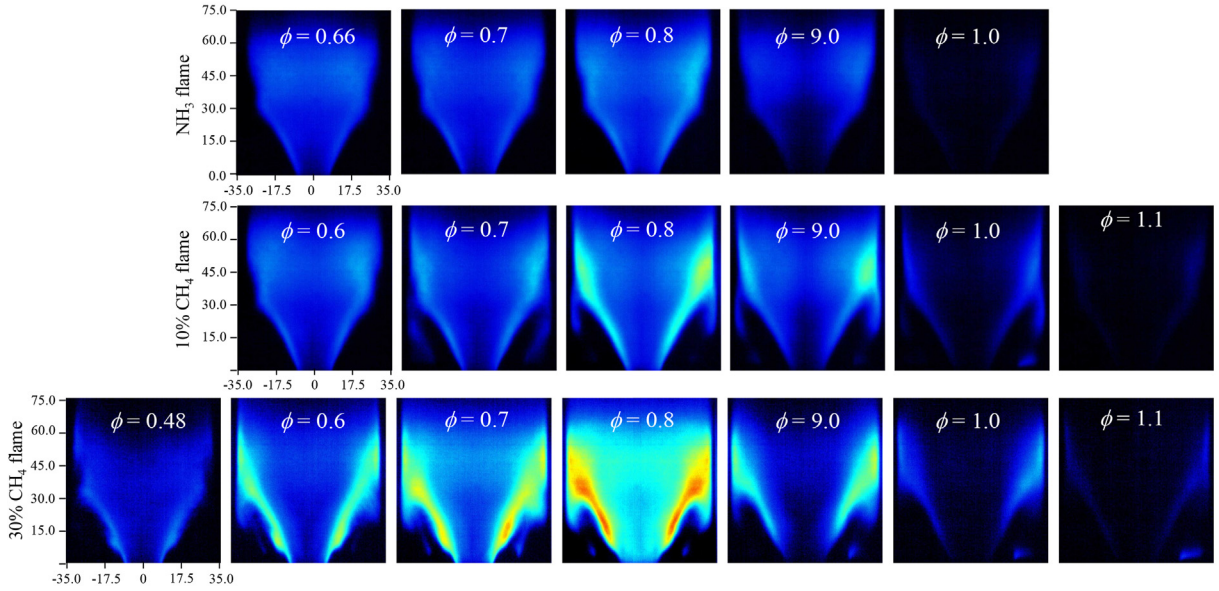

(b)

Fig. 4 – (a) The instantaneous OH-PLIF images; (b) the time averaged OH-PLIF images of 500 single shots. Top row: NH_3 flame; middle row: 10%CH_4 flame; bottom row: 30%CH_4 flame. OH-PLIF images are taken within the red dashed box shown in the digital image in Fig. 3. (For interpretation of the references to colour in this figure legend, the reader is referred to the Web version of this article.)

When viewing Fig. 5, it can be observed that the OH intensity is slightly increased at lean conditions when adding 10% methane. In comparison, 10% hydrogen addition barely influences I_{ave} while only switches the φ corresponding to the peak value of I_{ave} to leaner condition. From flame stabilization point of view, small amount of methane addition increases the laminar flame speed S_L and heat release rate HRR, as shown in Fig. 6. And the enhancement is more evident for hydrogen addition. As analysed in the literature [3,7], the poor flame stabilization feature of NH_3 flame is mainly attributed to the extremely low laminar flame speed and heat release rate. This means that 10% methane or hydrogen addition shows a

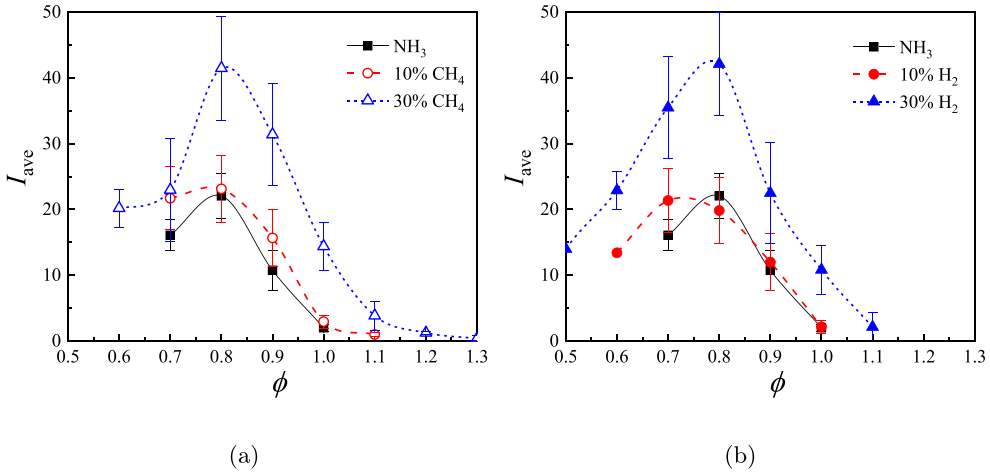

Fig. 5 – The relationship of the plane-integrated time-averaged OH-PLIF intensity I_{ave} with equivalence ratio for NH_3/CH_4/air and NH_3/H_2/air flames. The mean value is obtained from 500 instantaneous OH-PLIF images and the error bars represent the deviation from the mean value.

pronounced ability to enhance the flame stabilization without largely increasing the NO emission. The results of Figs. 5 and 6 indicates there exists great potential of ammonia application in gas turbines when the combustion is manipulated by the small molecular active fuels like methane or hydrogen. In the other words, the flame can be strengthened without increasing the NOx emissions by adding small amount of methane or hydrogen. However, the I_{ave} is largely increased for both 30%CH_4 flame and 30%H_2 flame, indicating NO emission would be largely increased. To quantitatively show the methane and hydrogen addition effect on emissions, next section examines main emissions measured with FTIR.

Emission of ammonia/air flame

Firstly, the NOx and NH_3 emission are analysed with 1D laminar flame simulation carried out by CHEMKIN-PRO [25] with the mechanism developed by Okafor et al. [24] for ammonia NH_3/CH_4/air flame. This mechanism was verified to well capture the flame speed and ignition time as well as emission characteristics at various conditions [14,27]. The emissions in the product gas is evaluated at the post flame where the species reaches a steady value. Typically, it is the end point, i.e. 5 cm, in the current study. Fig. 7 shows the variations of NO, NO_2, N_2O and NH_3 with the equivalence ratio φ. As shown in the figure, the readily high NO concentration is seen for $\varphi < 1.1$. From lean condition to $\varphi = 1.1$, the NO concentration firstly increases and then decreases with equivalence ratio φ and the peak value, about 4200 ppm, is obtained at $\varphi \approx 0.9$. For the rich flame of $\varphi > 1.15$, NO concentration is below 150 ppm which is significantly small compared with the lean conditions. However, the unburned NH_3 in exhaust gas dramatically increases with equivalence ratio when $\varphi > 1.15$ while no NH_3 is seen when $\varphi < 1.15$. It should be noted that the order of NO and NH_3 mole fractions are the same around $\varphi \approx 1.15$, which can be regarded as optimal operating condition for pure ammonia combustion. This suggests the possible composition of fuel and air for low emission of the NH_3 flame.

As proposed in recent study [27], to realize the application of ammonia fuelled in gas turbines, simultaneous reduction of

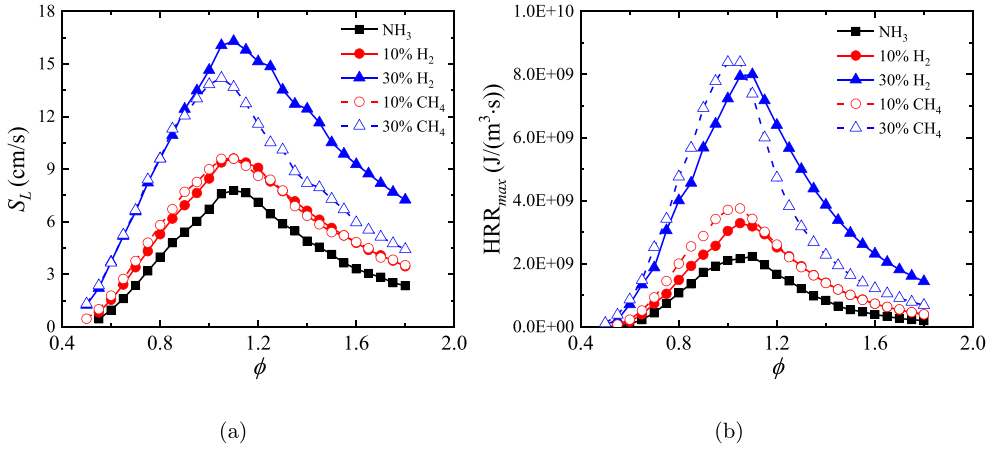

Fig. 6 – The laminar flame speed S_L and the maximum heat release rate obtained from one-dimensional laminar flame calculated by CHEMKIN PRO.

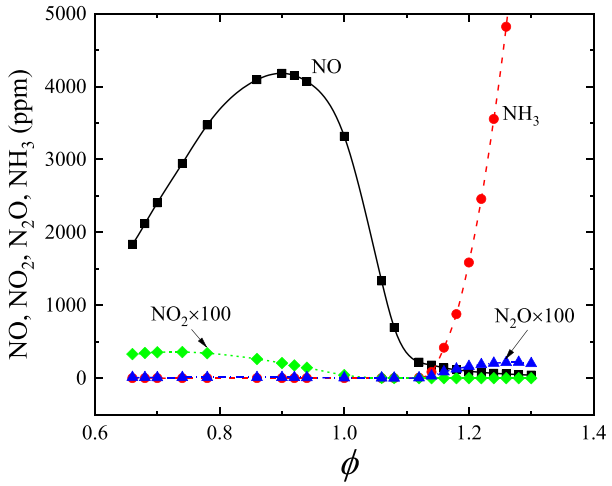

Fig. 7 – The concentrations of the main emissions obtained from the one-dimensional NH_3 flame.

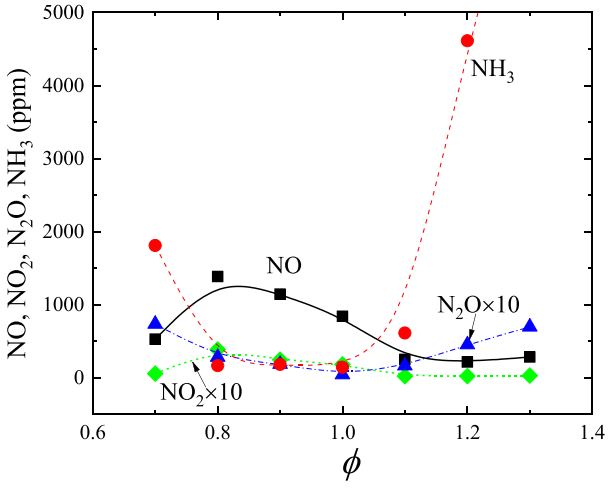

Fig. 8 – The concentrations of the main emissions obtained from the NH_3 swirl flame.

NOx and unburnt NH_3 is essential. Therefore, we next investigate the emission characteristics of the swirl flame by analysing the exhaust gas measured by FTIR. The emissions of the NH_3 flame in the model swirl combustor are shown in Fig. 8. We can see a similar trend of the measured NOx and unburned NH_3 emissions as 1D simulation results even through the values are not exactly matched with 1D flame due to the swirl flow and combustor wall heat loss. For lean conditions, NH_3 emissions are mostly due to the quenching caused by deficient combustion intensity. Therefore, the flame emits relatively high NH_3 emission at $\varphi = 0.7$ due to the flame local quenching since it is close to the blow-off limit. Similar to the 1D laminar flame, large NO emission is seen when $\varphi < 1.05$. The maximum NO concentration reaches about 1500 ppm at $\varphi \approx 0.8$ and starts to decrease when φ is beyond 0.8. No apparent NO emission is detected when $\varphi > 1.1$. Furthermore, due to the excessive fuel supply, the unburned NH_3 concentration is significantly increased when $\varphi > 1.05$ and out of the measuring range (5000 ppm) for $\varphi > 1.25$.

We can also concluded from Fig. 8 that NO is the main source for NOx emission. Therefore, the main propose should be controlling NO and unburned NH_3 for ammonia combustion. It can be seen that NO and NH_3 concentrations can be simultaneously decreased to a lower value at φ approximately 1.1, indicating the realizability of fuelling ammonia in a practical gas turbine combustor. In addition, it is possible to reduce NOx and unburned NH_3 simultaneously by adopting additional selective catalytic reduction (SCR), which satisfying the government regulations.

Effects of methane/hydrogen addition on the emissions

As mentioned in the earlier section and Ref. [8], the flame stabilization can be enhanced by adding active fuels like methane/hydrogen since the laminar flame speed is increased. However, this brings the high emission issue, i.e., high NOx emissions. Fig. 9 shows NO, NO_2 and N_2O concentration in the exhausted gas for the methane and hydrogen regulated ammonia flames. The emissions of pure ammonia flame are also plotted for comparison purposes. We first analyze the conditions with the blending ratio of 0.1. It can be observed that the behavior of NO and NO_2 emissions with equivalence ratio of the 10%H_2 flames are similar to the NH_3 flames. The peak value of NO is slightly lower and the corresponding equivalence ratio goes to richer condition. This indicates that the NH_3 flame can be regulated through adding a small amount of hydrogen without increasing the NOx emission level since NO is a major source of NOx emission. For the 10%CH_4 flames, NO emission is higher than that of the NH_3 flames when $\varphi < 1.05$. At fuel rich condition ($\varphi > 1.05$), NO emission seems to reach the same amount as the NH_3 flames. In addition, NO concentration is about twice as the 10%H_2 flames at $\varphi \leq 0.8$ and the difference becomes smaller as the mixture towards richer. When viewing NO_2, a similar trend is observed. NO_2 concentration of 10%CH_4 flame is also about two times larger than 10%H_2 flames when $\varphi < 0.9$. It can be readily seen that at fuel rich condition ($\varphi > 1.05$) NO concentration is very low (~100 ppmv) for the NH_3 flames, 10%CH_4 flames and 10%H_2 flames, indicating the possible operating condition for ammonia fuelled gas turbines. Moreover, for both pure ammonia flames and the co-firing flames, it can be seen that N_2O emission is mainly produced in fuel lean conditions and monotonously decreases. At the blending ratio of 0.1, methane and hydrogen addition show nearly the same effect on N_2O emission.

When the blending ratio is 0.3, the NO and NO_2 emissions increases significantly for both flames. The peak value of the NO emission from the 30%H_2 flame is more than 2000 ppmv at the $\varphi \approx 0.9$. It should be noted that the measured of NO concentration of the 30%CH_4 flames is about several times larger than the NH_3 flames at similar conditions. Therefore, to realize the ammonia fulled gas turbines, the combustion performance can not be improved by solely increasing the methane/hydrogen ratio in the fuel. There may exist an optimal blending ratio for each condition to compromise the flame stabilization and the combustion emission.

The O, H and OH radicals concentration during the combustion is crucial to influence the NO formation since fuel NOx production is a main source when ammonia is burned. NO is

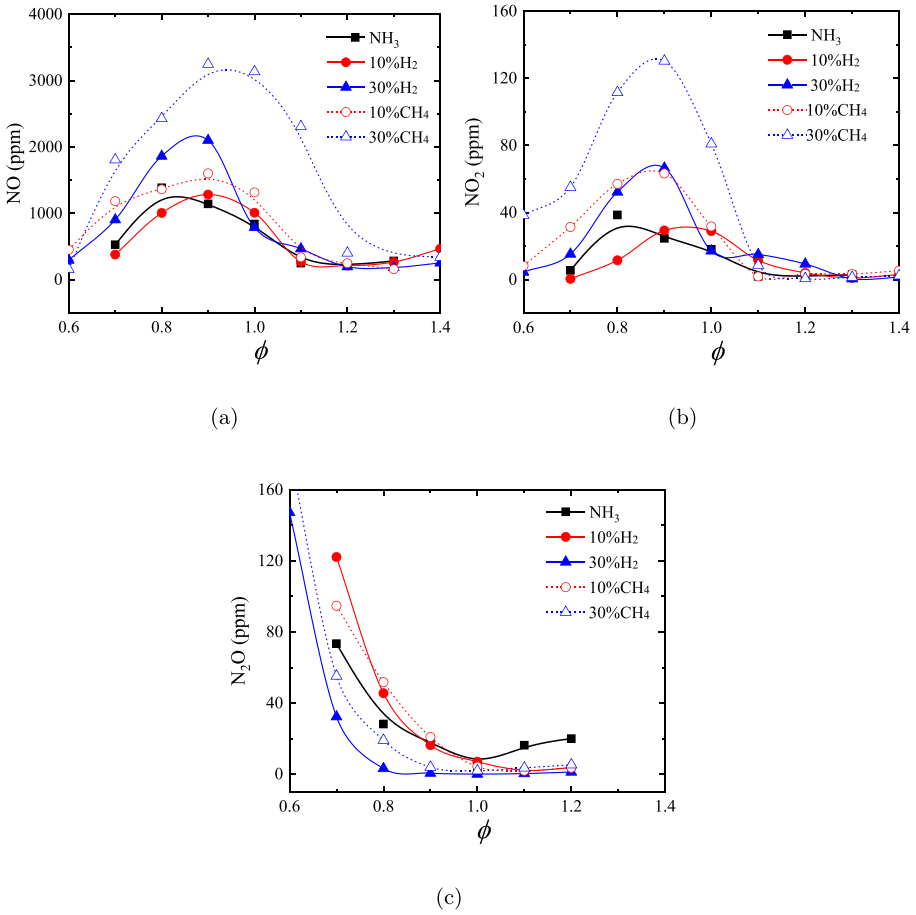

Fig. 9 – The NOx emissions with equivalence ratio for different swirl flames.

produced through the HNO intermediate, resulting from the oxidation of NH_i by O, H and OH radicals [29,30]. Hence, fuel NO production is sensitive to the concentration of the OH radicals. When the flame is rich, the OH concentration is low, which may lead to low NO emission at rich conditions. On the other hand, the lower NO emission from rich ammonia flames may be due to the promotion of a pathway that does not involve NO production. There is another pathway for $NH_2 \rightarrow N_2$ conversion at rich conditions to reduce NO emission $NH_2 + NH \rightarrow N_2H_2 + M$, $H \rightarrow NNH \rightarrow N_2$. N_2O is produced mainly through the reactions of NO with NH and with HO_2. On the other hand, N_2O is large consumed mainly through reaction with H radicals and through thermal dissociation. The consumption of N_2O is therefore suppressed at low temperatures and low concentration of H radicals which are typical conditions in far-lean equivalence ratios, as shown in Fig. 9(c).

The CO and CO_2 emissions from the flames are illustrated in Fig. 10. The figure shows that the measured CO emission increases rapidly with the equivalence ratio when $\varphi > 1$ and increases with the methane content in the fuel. This is due to the fact that CO comes from the incomplete combustion of the excessive methane for $\varphi > 1$ and the excessive CH_4 is increasing with the blending ratio. Higher CO emission in fuel rich conditions indicates lower combustion efficiency. It can be clearly seen that CO_2 emission is zero for NH_3 and hydrogen blending flames, showing a carbon free combustion process. When methane is added, the CO_2 increases with methane content at lean conditions due to the increasing carbon contained in methane. However, CO_2 emission largely increases when $\varphi > 1.1$ for $Z_{CH_4} = 0.1$, which is larger than that of $Z_{CH_4} = 0.3$. The smaller concentration of CO for $Z_{CH_4} = 0.3$ may be due to the increasing unburned CO.

The LES study on NOx emission

To further reveal the relationship of temperature, NO and OH field for methane addition flames, LES with detailed chemistry is performed in this study. Fig. 11 shows the comparison of radial profiles of mean axial and azimuthal velocity between LES and PIV measurements. The simulation shows a good prediction capability and the proper specifications of the boundary conditions of the current model, by comparing the velocity profile. The simultaneous instantaneous NO and OH distributions from LES at the center plane of the burner are shown in Fig. 12(a). It also can be seen that the local regions of relatively high OH intensity corresponds to regions of relatively high NO intensity. In addition, Fig. 12(b) shows the correlations of NO and OH at the slice shown in Fig. 12(a). It is clear to see that the intermediate radical NO and OH exhibits a general positive correlation even through it is scattered. This

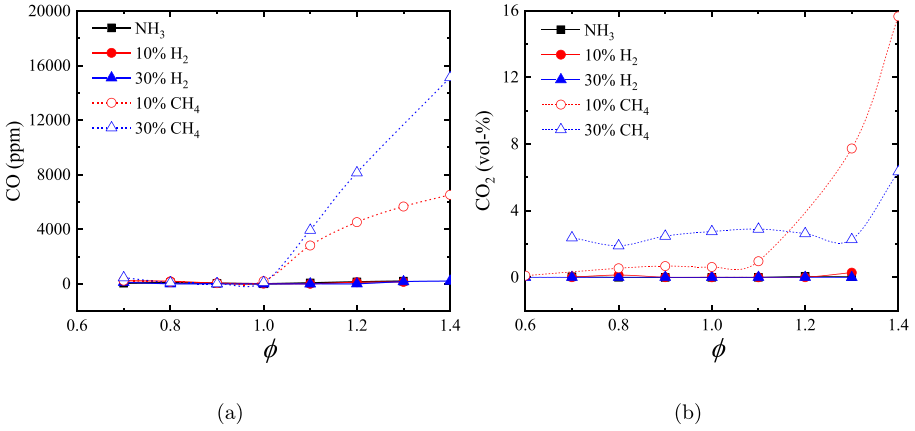

Fig. 10 – The CO and CO_2 emission of the NH_3/CH_4/air and NH_3/H_2/air swirl flame.

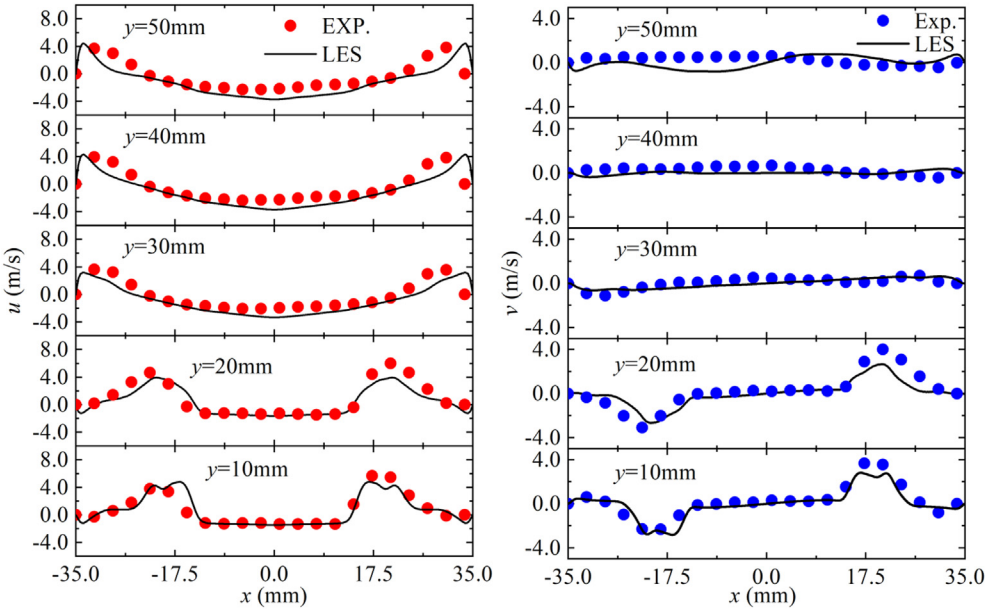

Fig. 11 – Comparison of radial profiles of mean axial and azimuthal velocity between LES and PIV measurements for NH_3 flame at $\varphi = 0.7$ and U = 4 m/s. Line: numerical results; symbols: experimental data.

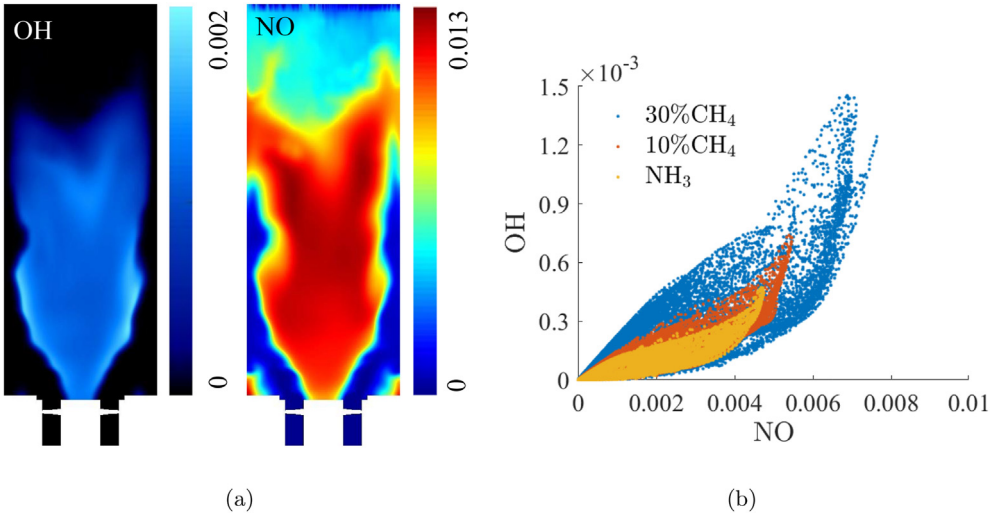

Fig. 12 – (a)Instantaneous distributions of NO and OH mass fraction of the NH_3 flame in the combustor, (b) the relation of the local NO and OH mass fraction. The flame is operated at $\varphi = 0.7$ and $U = 5$ m/s.

also verifies the plane-integrated time-averaged OH intensity can be a proper parameter to show the NO emission behavior in the earlier section.

In Fig. 9, it can be noted that the NO concentration of lean condition is significantly larger than that of rich condition. To reveal the emission characteristics, we perform the LES for NH_3/CH_4/air flames at $\varphi = 0.7$ with different blending ratios of $Z_{CH_4} = 0$, 0.1, 0.3. Fig. 13 shows the temperature, the instantaneous intermediate radicals of NO, OH and the emission of N_2O, NO_2, H_2, CO, CO_2 for different Z_{CH_4}. As inspecting the 2D temperature, OH and NO profile, the high OH concentration is seen in the high gradient location of temperature, which indicates the chemical reaction region since the flamelet concept is assumed. For the hydrocarbon flames, i.e. methane/air flame, temperature play a primary role for the NOx formation. In comparison, in ammonia containing flames, fuel NOx formation is a major source for the NOx emission, which results in the temperature playing a secondary role in promoting NOx

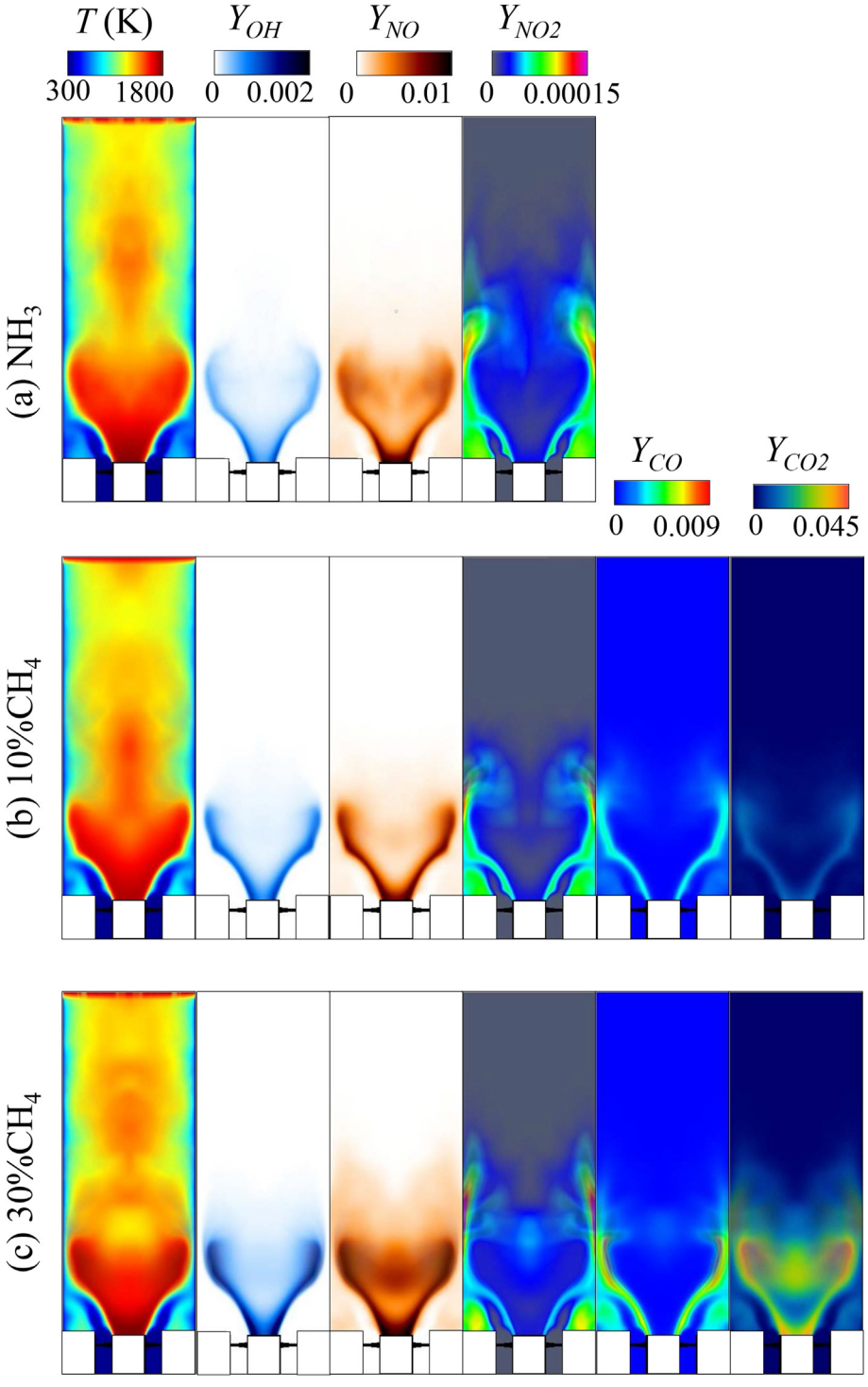

Fig. 13 – Two dimensional profile of the instantaneous intermediate species and the emissions of CH_4/NH_3 co-firing flame at $Z_{CH_4} = 0$, 0.1, 0.3. Y represents the mass fraction.

formation. From Fig. 13, it can be observed that the temperature is close for each flames in the combustion chamber, while the NO emission increases significantly with the amount of methane addition into the fuel. However, the concentration of NO_2 shows decreasing behavior as the blending ration increases, which is consistent with the emission measurement in Fig. 9. It is also observed that large NO_2 concentration at outer recirculation zone and near-wall regions because the temperatures of those regions is lower.

By inspecting the intermediate species during the combustion, it can noted that the production of OH radicals is promoted by H_2 and CO consumption. Those two species (H_2 and CO) are mainly consumed through the chain-propagating reactions $CO + OH = CO_2 + H$ and $H_2 + OH = H + H_2O$, respectively. These two reactions facilitate O and OH production via the chain-branching reaction $H + O_2 = OH + O$, which results in O/H radical concentration increasing, as a consequence.

Conclusions

This study investigates the regulation effect of methane and hydrogen on the emission characteristics of the ammonia/air flames in a gas turbine combustor. The instantaneous OH profile and the global emissions at the combustion chamber outlet are measured with Planar Laser Induced Fluorescence (PLIF) technique and Fourier Transform Infrared (FTIR), respectively. Large eddy simulation using OpenFOAM is performed to further reveal the mechanism of emission production. The following conclusions are made:

1. The emission character from the gas turbine combustor and one-dimensional flame is compared. It is found that the emissions behavior of gas turbine combustor follows the similar trend, showing that the NOx emissions and the unburned NH_3 can be simultaneously controlled to a proper value at φ approximately 1.15.
2. When the blending ratio (Z_f) is 0.1, the variation of NO and NO_2 with φ for NH_3/H_2/air flames and NH_3/CH_4/air flames is similar to the NH_3 flames. This indicates that the NH_3 flame properties can be promoted through adding a small amount of active fuels without increasing the NOx emission level.
3. When $Z_f = 0.3$, large NOx and CO emission for NH_3/CH_4/air flames is observed due to the increasing of carbon in the fuel. Comparing with NH_3/CH_4/air flame, H_2 shows larger potential on regulating the flame properties and emission control for $Z_f < 0.3$.
4. NO and OH species exhibit a general positive correlation from the LES results. In ammonia containing flames, the temperature plays a secondary role in promoting NOx formation while it is mainly produced from fuel NOx formation.

Declaration of competing interest

The authors declare that they have no known competing financial interests or personal relationships that could have appeared to influence the work reported in this paper.

Acknowledgements

The This study is supported by the National Natural Science Foundation of China (No.51706172) and the Shaanxi Province Postdoctoral Science Foundation (3127100061). Meng Zhang acknowledges the joint research project with Xinjiang Uygur Autonomous Region Inspection Institute of Special Equipment (3211002769).

REFERENCES

[1] Valera-Medina A, Xiao H, Owen-Jones M, David W, Bowen P. Ammonia for power. Prog Energy Combust Sci 2018;69:63–102.
[2] Ikäheimo J, Kiviluoma J, Weiss R, Holttinen H. Power-to-ammonia in future north european 100% renewable power and heat system. Int J Hydrogen Energy 2018;43(36):17295–308.
[3] Okafor EC, Somarathne KKA, Hayakawa A, Kudo T, Kurata O, Iki N, Kobayashi H. Towards the development of an efficient low-NOx ammonia combustor for a micro gas turbine. Proc Combust Inst 2019;37(4):4597–606.
[4] Kobayashi H, Hayakawa A, Somarathne KKA, Okafor EC. Science and technology of ammonia combustion. Proc Combust Inst 2019;37(1):109–33.
[5] Valera-Medina A, Marsh R, Runyon J, Pugh D, Beasley P, Hughes T, Bowen P. Ammonia–methane combustion in tangential swirl burners for gas turbine power generation. Appl Energy 2017;185:1362–71 [clean, Efficient and Affordable Energy for a Sustainable Future].
[6] Li S, Zhang S, Zhou H, Ren Z. Analysis of air-staged combustion of NH3/CH4 mixture with low NOx emission at gas turbine conditions in model combustors. Fuel 2019;237:50–9.
[7] Hayakawa A, Arakawa Y, Mimoto R, Somarathne KKA, Kudo T, Kobayashi H. Experimental investigation of stabilization and emission characteristics of ammonia/air premixed flames in a swirl combustor. Int J Hydrogen Energy 2017;42(19):14010–8.
[8] Zhang M, Wei X, Wang J, Huang Z, Tan H. The blow-off and transient characteristics of co-firing ammonia/methane fuels in a swirl combustor. Proceedings of the Combustion Institute Inpress 2020. https://doi.org/10.1016/j.proci.2020.08.056.
[9] Okafor EC, Somarathne KA, Ratthanan R, Hayakawa A, Kudo T, Kurata O, Iki N. Taku, Control of nox and other emissions in micro gas turbine combustors fuelled with mixtures of methane and ammonia. Combust Flame 2020;211:406–16.
[10] Lee J, Kim J, Park J, Kwon O. Studies on properties of laminar premixed hydrogen-added ammonia/air flames for hydrogen production. Int J Hydrogen Energy 2010;35(3):1054–64.
[11] Cai T, Zhao D, Wang B, Li J, Guan Y. NOx emission and thermal performances studies on premixed ammonia-oxygen combustion in a CO2-free micro-planar combustor. Fuel 2020;280:118554.
[12] Zhang M, An Z, Wei X, Wang J, Huang Z, Tan H. Emission analysis of the CH4/NH3/air co-firing fuels in a model combustor. Fuel 2021;291:120135.
[13] Glarborg P, Miller JA, Ruscic B, Klippenstein SJ. Modeling nitrogen chemistry in combustion. Prog Energy Combust Sci 2018;67:31–68.
[14] Okafor EC, Naito Y, Colson S, Ichikawa A, Kudo T, Hayakawa A, Kobayashi H. Measurement and modelling of

the laminar burning velocity of methane-ammonia-air flames at high pressures using a reduced reaction mechanism. Combust Flame 2019;204:162–75.
[15] Jójka J, Ślefarski R. Dimensionally reduced modeling of nitric oxide formation for premixed methane-air flames with ammonia content. Fuel 2018;217:98–105.
[16] Ramos CF, Rocha RC, Oliveira PM, Costa M, Bai X-S. Experimental and kinetic modelling investigation on NO, CO and NH3 emissions from NH3/CH4/air premixed flames. Fuel 2019;254:115693.
[17] Zhang M, Chang M, Wang J, Huang Z. Flame dynamics analysis of highly hydrogen-enrichment premixed turbulent combustion. Int J Hydrogen Energy 2020;45(1):1072–83.
[18] Zhang W, Wang J, Lin W, Guo S, Zhang M, Li G, Ye J, Huang Z. Measurements on flame structure of bluff body and swirl stabilized premixed flames close to blow-off. Exp Therm Fluid Sci 2019;104:15–25.
[19] Huang Y, Yang V. Dynamics and stability of lean-premixed swirl-stabilized combustion. Prog Energy Combust Sci 2009;35(4):293–364.
[20] Zhang W, Wang J, Lin W, Li G, Hu Z, Zhang M, Huang Z. Effect of hydrogen enrichment on flame broadening of turbulent premixed flames in thin reaction regime. Int J Hydrogen Energy 2021;46(1):1210–8.
[21] Guo S, Wang J, Wei X, Yu S, Zhang M, Huang Z. Numerical simulation of premixed combustion using the modified dynamic thickened flame model coupled with multi-step reaction mechanism. Fuel 2018;233:346–53.
[22] Guo S, Wang J, Zhang W, Lin B, Wu Y, Yu S, Li G, Hu Z, Huang Z. Investigation on bluff-body and swirl stabilized flames near lean blowoff with PIV/PLIF measurements and LES modelling. Appliled Thermal Engineering 2019;160:114021.
[23] Xiao H, Howard M, Valera-Medina A, Dooley S, Bowen PJ. Study on reduced chemical mechanisms of ammonia/methane combustion under gas turbine conditions. Energy Fuels 2016;30(10):8701–10.
[24] Okafor EC, Naito Y, Colson S, Ichikawa A, Kudo T, Hayakawa A, Kobayashi H. Experimental and numerical study of the laminar burning velocity of CH4/NH3/air premixed flames. Combust Flame 2018;187:185–98.
[25] CHEMKIN-PRO 17.2, San Diego: ANSYS, Inc.; 2016.
[26] Hayakawa A, Goto T, Mimoto R, Kudo T, Kobayashi H. No formation/reduction mechanisms of ammonia/air premixed flames at various equivalence ratios and pressures. Mechanical Engineering Journal 2015;2(1). 14–00402–14–00402.
[27] Somarathne KDKA, Okafor EC, Hayakawa A, Kudo T, Kurata O, Iki N, Kobayashi H. Emission characteristics of turbulent non-premixed ammonia/air and methane/air swirl flames through a rich-lean combustor under various wall thermal boundary conditions at high pressure. Combust Flame 2019;210:247–61.
[28] Zhang M, Wang J, Wu J, Wei Z, Huang Z, Kobayashi H. Flame front structure of turbulent premixed flames of syngas oxyfuel mixtures. Int J Hydrogen Energy 2014;39(10):5176–85.
[29] Miller J, Smooke M, Green R, Kee R. Kinetic modeling of the oxidation of ammonia in flames. Combust Sci Technol 1983;34(1–6):149–76.
[30] Somarathne KDKA, Hatakeyama S, Hayakawa A, Kobayashi H. Numerical study of a low emission gas turbine like combustor for turbulent ammonia/air premixed swirl flames with a secondary air injection at high pressure. Int J Hydrogen Energy 2017;42(44):27388–99.